J. Water Environ. Nanotechnol., 6(3): 212-223 Summer 2021

ORIGINAL RESEARCH PAPER

Removal of Cu(II) from water using Succinic Anhydride functionalized TiO_2 nanoparticles

Ananta Saikia[1,2], Binoy K. Saikia[3], Pranjal Saikia[1*]

[1] Department of Applied Sciences (Chemical Science Division), Gauhati University, Guwahati-781014, Assam, India
[2] Defence Research Laboratory, Tezpur-784001, Assam, India
[3] CSIR-North East Institute of Science & Technology, Jorhat-785006, Assam, India

Received: 2021-05-14 Accepted: 2021-06-15 Published: 2021-07-01

ABSTRACT

Removal of heavy metals from wastewater is a need of the hour. Titanium dioxide (TiO_2) nanoparticles were functionalized using succinic anhydride (SA) and adsorption of copper (II) on SA functionalized TiO_2 nanoparticles (TiOSA) was carried out. The adsorption of Cu (II) on TiOSA was estimated concerning pH, contact time, and adsorbent dose. The study confirms the best removal of Cu (II) using the said adsorbent is at pH 8. The Cu (II) concentration can be reduced to less than 1.1 mg/L at a contact time of 180 min with an initial 15 mg/L Cu (II) concentration using the adsorbent dose of 0.6 g/50 mL. The study reveals that the adsorption process preferably follows the Langmuir isotherm model. Also, the thermodynamic parameters like entropy change (ΔS°), enthalpy change (ΔH°), and free energy change (ΔG°) were calculated for the adsorption process. The pseudo-second-order kinetic model was found to be better fitted to the adsorption.

Keywords: *Succinic anhydride, Functionalization, Titanium dioxide, Removal of Cu(II), Water.*

How to cite this article
Saikia A., Saikia B.K., Saikia P. Removal of Cu(II) from water using Succinic Anhydride functionalized TiO_2 nanoparticles . J. Water Environ. Nanotechnol., 2021; 6(3): 212-223.
DOI: 10.22090/jwent.2021.03.002

INTRODUCTION

Water is essential for all dimensions of life. We can survive for about 20 days without food, but without water, we cannot even survive for few days [1]. Apart from being the basic requirement, clean and safe water has also a great influence on all the aspects of human life [2, 3]. As water is the most taken drinking fluid, it is considered a potential source of disease transmission, especially in developing countries. According to the World Health Organization (WHO), 80% of diseases in developing countries are water-borne [4].

Contamination of heavy metals in the environment is mainly due to the rapid escalation of industrialization towards a developed society. The waste products generated from the textiles, chemicals, mining, and metallurgical industries are mainly responsible for water contamination [5-6]. Heavy metal pollution has greatly threatened human health and the natural ecosystems even at low concentrations. Because they are non-biodegradable, their presence in drinking water is a public health problem due to their possible accumulation in organisms [7-9]. Heavy metals may accumulate in living tissues causing metabolic and physiological problems leading to different health issues [10-13]. To address these problems, in the recent decade, a tremendous amount of research has been done to identify robust methods of purifying water at lower cost, with less energy and minimum impact on the environment [14, 15]. To protect human health and the environment, it is necessary to remove heavy metals from various industrial wastewaters before discharging them to

* Corresponding Author Email: *pranjalsaikia@gauhati.ac.in, saikiaananta@yahoo.com*

the environment. Till now, several technologies have been developed for the removal of heavy metal ions from water and wastewater, including chemical precipitation [16], ion exchange [17-18], liquid-liquid extraction [19], electrodialysis [20], biosorption [21-23], adsorption [24-26], membrane filtration, coagulation, flocculation [27- 28] and so on. Out of these, adsorption is considered one of the most effective methods owing to its high removal efficiency, low cost, ease of operation, and reusability [29-30]. Some typical adsorbents employed in heavy metal ion adsorption includes activated carbon [31-32], zeolites [33], clay [34], graphene [35], carbon nanotubes (CNTs) [36], bioadsorbents [37, 38], and various metal oxides [39]. However, it is important to develop adsorbents which can remove contaminants quickly and can be recycled in order to achieve an efficient treatment system [40].

Recently, nano-scaled magnetic particles have been proposed as adsorbents for environmental decontamination [41-42]. Due to their unique chemical and physical properties, like high dispersibility, high surface-to-volume ratio, etc., they exhibit a high adsorption capacity [43]. Therefore, the concept of magnetic nanoparticles as adsorbents in water treatment processes has become increasingly popular [44-45]. Numerous cost-effective and environment-friendly nanomaterials have been developed for the decontamination of industrial effluents, groundwater, surface water, and drinking water. Among different kinds of nano-adsorbents, oxide-based nanomaterials such as Fe_3O_4, TiO_2, ZnO, and their composites are playing a more important role. Recently, there have been several reports on magnetic oxides, especially Fe_3O_4, being used as nano-adsorbents for the removal of various toxic metal ions from wastewater, such as Ni^{2+}, Cr^{3+}, Cu^{2+}, Cd^{2+}, Co^{2+}, Hg^{2+}, Pb^{2+} and As^{3+} [46-50].

In order to meet diverse requirements, nano-engineering of the surface of the nanoparticles is inevitable. Efforts have been made to tailor the surface properties (e.g., charge density, functionality, reactivity, biocompatibility, stability, and dispersibility), produce hollow nanostructured materials, and create multi-functional composite nanoparticles [51-55]. Nanoparticles functionalized with biocompatible organic/inorganic molecules [56], polymers, and dendrimers [57, 58] are more effective since the free functional groups present on the surface provide a large number of active sites for adsorption as well as aqueous stability, which is necessary for the efficient adsorption of toxic metal ions and bacterial pathogens [59-60].

With these backgrounds, in this work, TiO_2 nanoparticles have been functionalized with succinic anhydride (SA) and study have been carried out for the removal of Cu (II) from water varying different parameters to know the adsorption capacity as well as thermodynamic and kinetic behavior of the adsorption process.

MATERIALS AND METHODS

The as such used titanium dioxide (TiO_2) (~ 7 nm, TiO_2- Anatase, 95%) was from SRL (Sisco Research Laboratories Pvt. Ltd.). The succinic anhydride (SA) and toluene used were from Fluka (99% pure) and Pallav™ (99.5% pure), respectively. The copper (II) chloride dihydrate (99% pure) used for the preparation of the stalk solution was from Merck. All the equipment used during the experimental studies was calibrated as per standard procedures. The initial pH of the Cu (II) solutions was achieved to its desired level by using NaOH (0.1 M) and/or HCl (0.1 M) solutions as and when necessary and analyzed by Cyber scan pH 510 (Eutech) instrument. The concentration of Cu (II) was determined by using the ICP-MS instrument (Perkin Elmer Elan, SCIEX, DRC-II, Canada). FTIR spectra were measured by using Bruker Optic (model- ALPHA-T) FTIR spectrophotometer over the wavenumber range of 4000 to 400 cm^{-1} using KBr pellets; made in an approximate sample to KBr ratio of 1:200. The Zeiss Sigma 300 scanning electron microscope was used for SEM analysis.

Functionalization of TiO_2 nanoparticles with surface area 326 m^2/g has been done with succinic anhydride (SA) using toluene as solvent [61]. In the functionalization reaction, 5 g of TiO_2 was added to 400 mL of toluene and then heated up to 353 K. Then, 12.53 g of SA was dissolved in 100 mL of solvent and added slowly to the reaction mixture. The functionalization reaction was maintained in constant reflux condition for 5 h. The functionalized TiO_2 nanoparticles (TiOSA) were recovered from solvent by centrifugation and then washed with water 3-4 times and dried in the oven.

The adsorption experiments were carried out by batch method to obtain the rate and equilibrium data. Simultaneously, to compare the other parameters, two separate experiments were conducted one using control TiO_2 nanoparticles and another using TiOSA. The mixtures containing

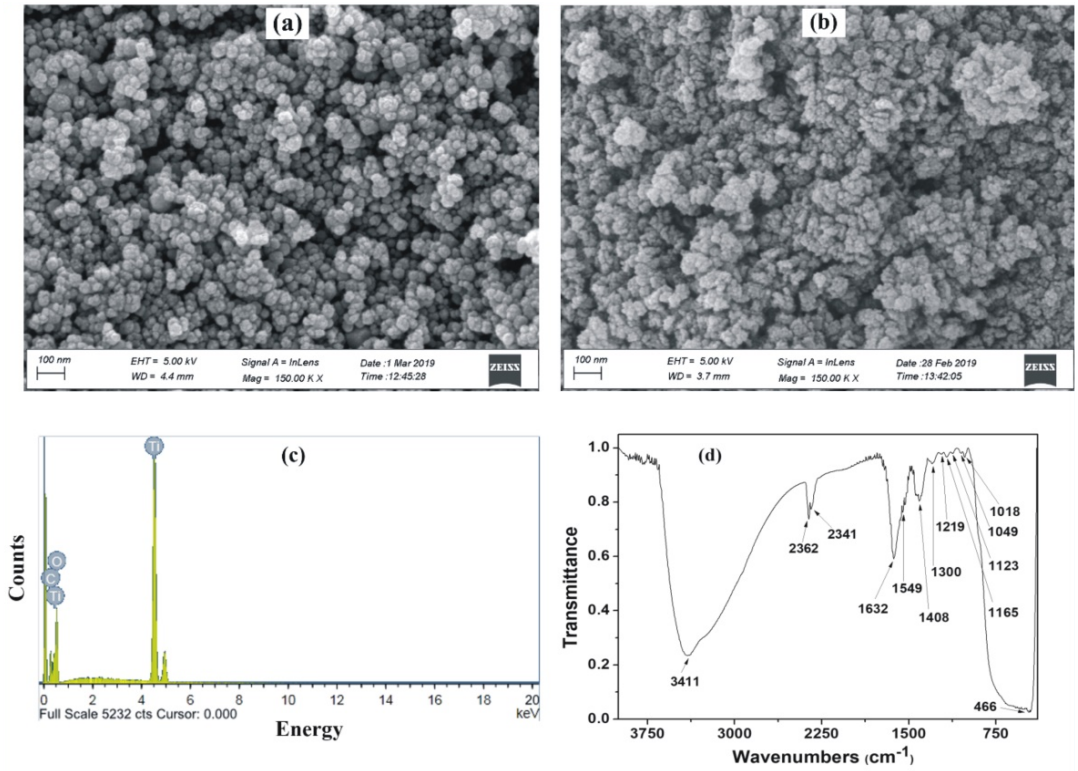

Fig. 1. (a) FE-SEM of TiOSA, (b) FE-SEM of TiOSA after Cu (II) adsorption (c) EDX of TiOSA, and (d) FTIR spectrum of TiOSA

50 mL known concentration of Cu (II) solutions and known quantities of adsorbents were shaken in a temperature-controlled orbital shaker at three different temperatures of 298, 303, and 308 K with a shaking speed of 175 rpm. The effect of the initial pH of the solutions on Cu (II) adsorption by the TiOSA was studied by using 15 mg/L of the adsorbent at various pH of the solutions. The adsorbent dose was varied from 0.15 to 0.6 g/50 mL to study the effect of adsorbent dose on adsorption, at pH 8 and constant contact time of 180 min with fixed (5 mg/L) Cu (II) concentration in spiked water. The study of the effect of contact time was carried out by varying contact time from 60 to 360 min at constant pH and adsorbent dose. The effect of initial Cu (II) concentration was studied at various adsorbent doses by varying initial Cu (II) concentration from 5 to 25 mg/L at pH 8 with a constant contact time of 180 min. The adsorption isotherm study was performed by using 0.45 g of TiOSA with 50 mL spiked water at different initial Cu (II) concentrations. Similarly, the study of kinetic and thermodynamic parameters of the adsorption was done by conducting the experiments at different contact times (60, 120, 180, 240, 300, and 360 minutes) and three different temperatures (298, 303, and 308 K) close to the ambient temperature so that the temperatures could be maintained easily.

To perform the desorption study, initially prepared the saturated TiOSA by treating 0.45 g of TiOSA with 50 mL of 50 mg/L Cu (II) solution under agitation for about 3 h at a shaking speed of 175 rpm and then filtered the Cu (II) saturated TiOSA and subsequently dried in the oven at 373 K. About 0.15 g of Cu (II) saturated TiOSA was agitated for 3 h at a shaking speed of 175 rpm, separately with 50 mL of three different strengths NaOH solution (0.1, 0.3, and 0.5 M). Then Cu (II) concentrations in the separated aqueous phases were determined.

RESULTS AND DISCUSSION

The SA functionalized TiO_2 nanoparticles (TiOSA) have been characterized using SEM, EDX, and FTIR. The SEM images, EDX, and FTIR spectrum of TiOSA are shown in Fig. 1.

The smooth-edged SEM image of TiOSA (Fig. 1a) suggests the surface modification of TiO_2 nanoparticles and the particle sizes in the range

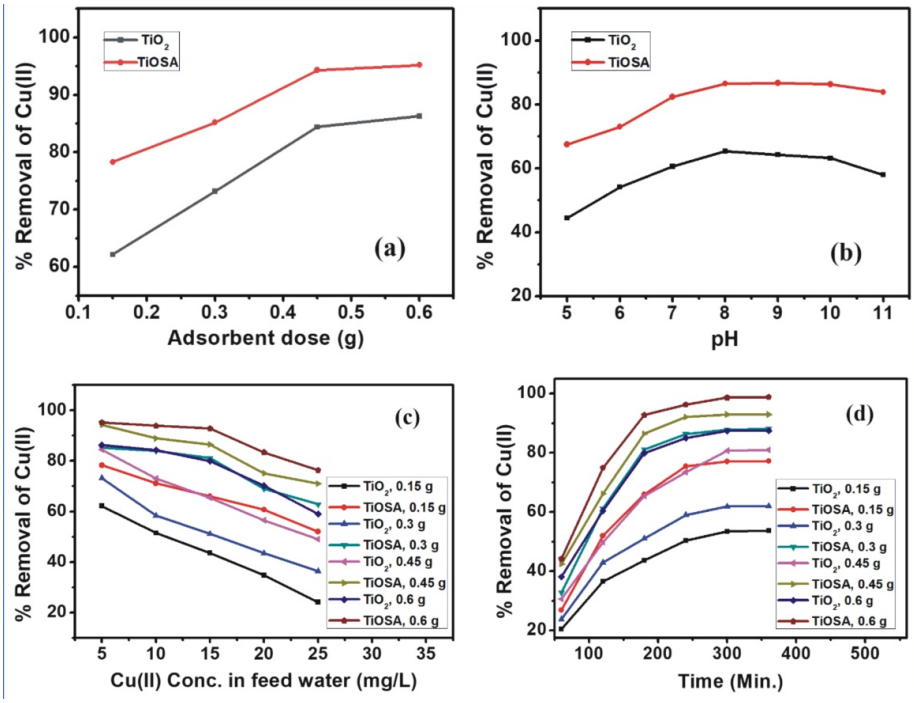

Fig. 2. (a) Effect of adsorbent dose on % removal of Cu (II), (b) Effect of pH on % removal of Cu (II), (c) Effect of initial ion concentration on % removal of Cu (II), and (d) Effect of contact time on % removal of Cu (II)

of 22-30 nm. As can be seen in Fig. 1b, the image became hazed and partially agglomerated reflecting the change in morphology of the particles after the adsorption of Cu (II) by TiOSA. The analysis of the EDX pattern (Fig. 1c) confirms the presence of Ti, C, and O in the TiOSA sample, which implies the surface modification with succinic anhydride (SA). In the FTIR spectra (Fig. 1d), the peak at 3411 cm^{-1} is due to the stretching vibration bands of –OH of absorbed water molecule [62]. The peak observed at 1632 cm^{-1} corresponds to the bending mode of Ti-OH [63]. The peak at 1549 cm^{-1} is due to –COO vibration [61]. The peak at 1219 cm^{-1} is for the bending vibration of the C-H bond [61]. The band corresponding to C-O-Ti was observed at 1165 cm^{-1} [61]. The peaks at1408 and 1049 cm^{-1} are due to C-O stretching vibrations [26]. A broad absorption band between 500 and 1000 cm^{-1} is attributed to the vibration of Ti-O-Ti [64].

The effect of adsorbent dose on adsorption of Cu (II) on TiOSA is depicted in Fig. 2a. The study revealed that adsorption of Cu (II) from the solution increases rapidly with an increase in adsorbent dose from 0.15-0.45 g/50 mL, after which a marginal increase is observed on further increase in the adsorbent dose for both TiO_2 and TiOSA. Due to the functionalization of TiO_2 with succinic anhydride (SA), the density of electronegative oxygen atoms on the surface of the TiO_2 nanoparticles increases, and hence the TiOSA surface will have more electronegative adsorption sites to adsorb metal ions like Cu (II). Hence, the removal of Cu (II) by TiOSA is found to be more effective than that of TiO_2.

The study of the pH effect on adsorption of Cu (II) on TiOSA is carried out in the pH range of 5 to 11. The plot of pH vs % removal of Cu (II) (Fig. 2b) suggests that the efficiency of Cu (II) removal increases with increasing pH from 5 to 8 and after that, either marginal increase or decrease was observed. In the study, a maximum of 86.5% (for TiOSA) and 65.4% (for TiO_2) removal of Cu (II) was observed at pH 8 with feed water concentration 15 mg/L using 0.45 g adsorbent. The results revealed that both at lower and higher pH values than 8, the Cu(II) removal by TiOSA and TiO_2 were low. This may be due to the fact that, at low pH, hydroxonium ion and Cu (II) ions compete for adsorption sites and therefore adsorption is low. However, the TiOSA surface becomes more negative with increasing pH, making it easier for Cu (II) ions adsorption. Beyond optimum pH,

Table 1. Desorption study of TiOSA

Adsorbet adsorbed by adsorbent at saturated point (mg g^{-1})	Eluent used	Conc. of eluent (M)	Adsorbet eluted from 0.15g adsorbent (mg g^{-1})	Regeneracy of adsorbent (%)
2.3556	NaOH	0.1	0.754	32.01
2.3556	NaOH	0.3	0.989	41.99
2.3556	NaOH	0.5	1.769	75.42

a decrease in metal ion adsorption is due to the formation of soluble Cu (II) ions complexes [65].

The effect of initial ion concentration on adsorption of Cu (II) on TiOSA, was observed by plotting initial ion concentration against the % removal of Cu (II) as shown in Fig. 2c. From the figure, it is understood that adsorption efficiency is higher at lower initial Cu (II) concentration (5 mg/L) and with increasing initial Cu (II) concentration, a slow decrease in Cu (II) adsorption by TiOSA as well as TiO_2 were observed. The decrease in Cu (II) removal at higher initial concentration may be due to saturation of the active sites of the adsorbent by the Cu (II), due to which further increase in Cu (II) concentration is not leading to the significant increase in absorption [66-67].

The adsorption of Cu (II) on TiOSA was studied by varying the agitation time to know the effect of contact time, using feed water containing 15 mg/L of Cu (II) as shown in Fig. 2d. The study revealed that the adsorption efficiency increases with increasing the contact time and reaches nearly maximum removal at 180 min. The removal becomes nearly constant after 180 min for both the cases of TiOSA and TiO_2. This may be due to the fact that with time the adsorption site of the adsorbent became saturated by the adsorbate [68-69]. The feedwater containing 15 mg/L of Cu (II) was reduced by 92.8% at contact time 180 min with an adsorbent dose of 0.6 g/50 mL.

The desorption study results (Table 1) revealed that the trend of desorption percentage at different concentrations of NaOH is in the order 0.1 M < 0.3 M < 0.5 M. Desorption of Cu (II) was found to be maximum (75.42%) with 0.5 M NaOH solution. From the study, it is observed that the used TiOSA can be regenerated for further use.

The mechanism of Cu (II) adsorption on TiOSA was investigated by studying the pseudo-first-order, pseudo-second-order, and Elovich kinetic models.

The pseudo-first-order kinetic model [70] is expressed in linear form as:

$$\log(q_e - q_t) = \log q_e - \frac{K_1 t}{2.303} \quad (1)$$

Where; K_1 (1/min) = rate constant.

q_e (mg/g) = the amount of adsorbate adsorbed per unit mass of adsorbent at equilibrium.

q_t (mg/g) = the amount of adsorbate adsorbed per unit mass of adsorbent at time t.

t (min) = time.

To understand the fitness of the adsorption kinetic with pseudo-first-order kinetic model the $\log(q_e - q_t)$ vs t for various initial Cu (II) concentrations were plotted (shown in Fig. 3a). The K_1 values at five different initial Cu (II) concentrations were calculated from slopes of the respective linear plots and also the correlation coefficient (R^2) was computed (Table 2). The R^2 values of the above plot reveal that the adsorption is not better fitted to the Pseudo first-order kinetic model.

The linear equation of pseudo second-order kinetic model [71] is expressed as:

$$\frac{t}{q_t} = \frac{1}{K_2 q_e^{\,2}} + (\frac{1}{q_e})t \quad (2)$$

Where; K_2 (g/mg min.) = rate constant.

q_e (mg/g) = the amount of adsorbate adsorbed per unit mass of adsorbent at equilibrium.

q_t (mg/g) = the amount of adsorbate adsorbed per unit mass of adsorbent at time t.

t (min) = time.

The experimental value of q_e and K_2 of the pseudo-second-order equation was calculated from the plot of t/q_t vs t (Fig. 3b) for Cu (II) adsorption on TiOSA at different initial Cu (II) concentrations at 303 K. From the plot (Fig. 3b) the correlation coefficient, R^2 was computed which was higher than that observed for the pseudo-first-order model. It implies the better fitness of the pseudo-second-order kinetic model. The computed values of q_e, K_2, and R^2 are given in Table 2. The value of q_e increases with the increase in initial Cu (II) concentration;

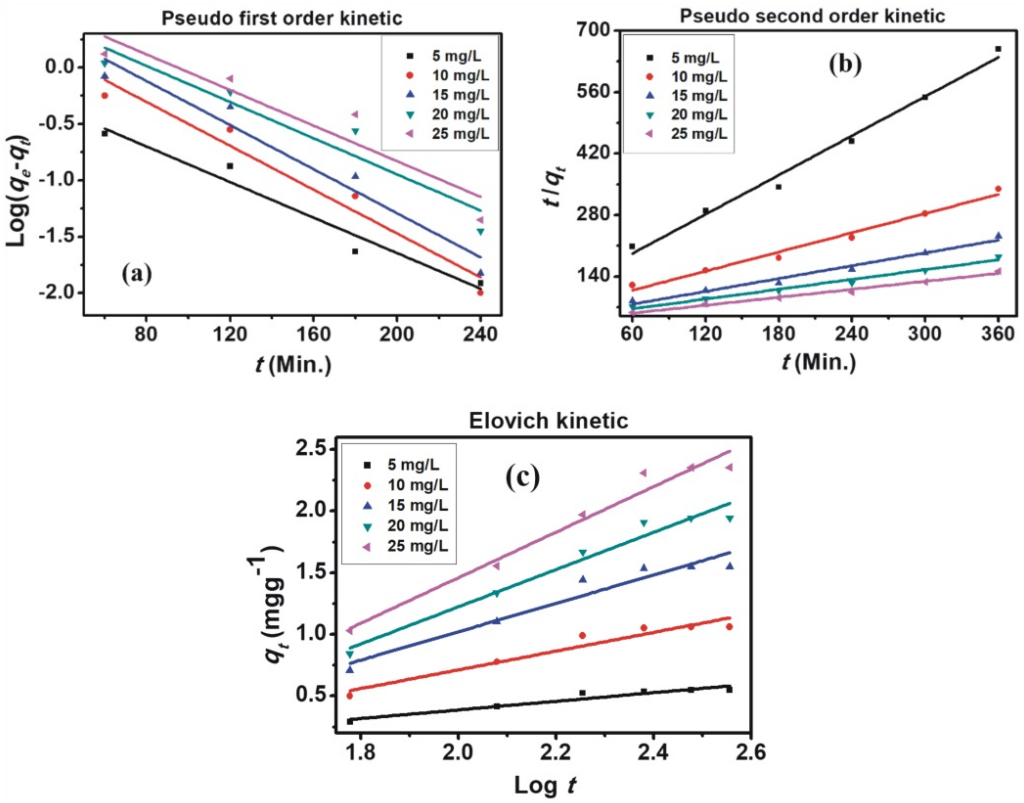

Fig. 3. (a) Pseudo first-order kinetic model, the plot between log (q_e-q_t) vs time, (b) Pseudo second-order kinetic model, the plot between t/q_t vs time, and (c) Elovich kinetic model plot between Log t vs q_t

Table 2. Kinetic parameters for the adsorption of Cu (II) on TiOSA

C_o (mg/ L)	q_e(mg/g)	Pseudo first order kinetic model			Pseudo second order kinetic model			Elovich kinetic model		
		K_1 (1/min)	q_e(mg/g)	R^2	K_2 [g/(mg min)]	q_e (mg/g)	R^2	α [mg/(g min)]	β (g/mg)	R^2
5	0.55	0.019	0.853	0.962	0.022	0.67	0.989	0.366	0.35	0.925
10	1.06	0.022	2.975	0.956	0.008	1.37	0.982	0.114	0.76	0.934
15	1.55	0.023	4.593	0.953	0.005	2.05	0.978	0.067	1.15	0.935
20	1.94	0.019	4.544	0.913	0.003	2.69	0.984	0.043	1.51	0.967
25	2.36	0.018	5.622	0.888	0.002	3.30	0.984	0.033	1.85	0.970

this may be due to the higher availability of Cu (II) to adsorb at a higher initial concentration. The values of rate constants, K_2 decrease with an increase in initial Cu (II) concentration which indicates the saturation of the TiOSA with Cu (II) at a higher initial concentration.

The Elovich model [72] is expressed by the equation:

$$\frac{dq_t}{d_t} = \alpha \exp(-\beta q_t) \quad (3)$$

Where; α (mg/(g min) = Elovich coefficients representing initial adsorption rate.

β (g/mg) = the adsorption coefficient.

Assuming $\alpha\beta t >> 1$ and applying the boundary conditions $q_t = 0$, $t = 0$ and $q_t = q_t$ at $t = t$, the simplified equation can be expressed as:

$$q_t = \beta \log(\alpha\beta) + \beta \log t \quad (4)$$

Elovich's kinetic model was studied by plotting Log t vs q_t as displayed in Fig. 3c. The constant β and the initial adsorption rate α were calculated from the slopes and intercepts of the plots. The

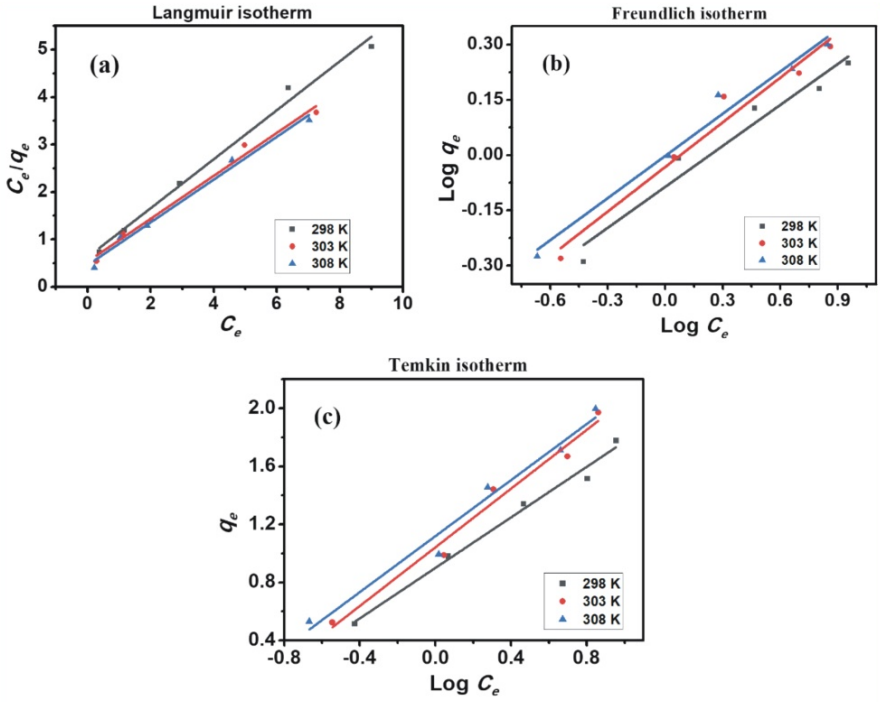

Fig. 4. (a) Langmuir isotherm, plot of C_e/q_e vs C_e, (b) Freundlich isotherm, plot of log q_e vs log C_e and (c) Temkin isotherm, plot of q_e vs log C_e

results with the correlation coefficients are given in Table 2. Comparatively low correlation coefficients (R^2) for the Elovich kinetic model reveal that this adsorption is not fitted with this kinetic model.

The three assumptions of Langmuir isotherm are; (i) the maximum adsorption corresponds to a saturated monolayer of adsorbate molecules on the adsorbent surface, (ii) the energy of adsorption is constant, and (iii) there is no transmigration of adsorbate molecules in the plane of adsorbent surface. The Langmuir adsorption isotherm [73] can be expressed as below:

$$q_e = \frac{q_m b C_e}{1 + b C_e} \quad (5)$$

Or $$\frac{C_e}{q_e} = \frac{1}{q_m} C_e + \frac{1}{q_m b}$$

Where; q_e (mg/g) = the amount of adsorbate adsorbed per unit mass of adsorbent.

C_e (mg/L) = the unabsorbed adsorbent concentration in solution at equilibrium condition.

q_m (mg/g) = the maximum amount of adsorbate adsorbed per unit mass of adsorbent to form a complete monolayer on the surface.

b (L/mg) = Langmuir constant.

The greater correlation coefficient (R^2) value in respect of the linear plot of C_e/q_e vs C_e (Fig. 4a) indicates the monolayer adsorption of Cu (II) on TiOSA. The values of q_m and b were calculated with the help of slope and intercept respectively and are presented in Table 3. The results showed that the maximum Cu (II) uptake (q_m) and the value of Langmuir constant (b) related to the affinity of the binding sites were increased with the increase of temperature. The highest R^2 value suggested that the process preferably followed the Langmuir isotherm model.

The Freundlich isotherm implies that the adsorbate adsorbs onto the heterogeneous surface of an adsorbent [74]. The isotherm can be applied to both monolayer (chemisorption) and multilayer adsorption (physisorption). The equation for a linear form of the Freundlich isotherm [75] is given below:

$$q_e = K_f C_e^{1/n} \quad (6)$$

Or $$\log q_e = \log K_f + \frac{1}{n} \log C_e$$

Where; q_e (mg/g) = the amount of adsorbate

Table 3. Parameters of adsorption isotherms for Cu (II) on TiOSA

		298°K	303°K	308°K
Adsorption isotherm	Adsorption parameters		Values	
Langmuir	q_m (mg/g)	1.9361	2.2092	2.21715
	b (L/mg)	0.8285	0.85455	0.98722
	R^2	0.99032	0.98834	0.98906
Freundlich	n	2.6969	2.47525	2.61965
	K_f [mg/g (L/mg)$^{1/n}$]	0.8199	0.92856	0.99479
	R^2	0.95722	0.96883	0.9781
Temkin	B	0.87068	1.01192	0.96578
	A(L/g)	10.83658	10.72818	7.81428
	b(kJ/mol)	2.84556	2.48947	2.65144
	R^2	0.9884	0.97787	0.97535

adsorbed per unit mass of adsorbent.

K_f [mg/g (L/mg)1/n] = a constant, sorption capacity of the adsorbent.

n = favourability of the adsorption process, constant related to the energy of intensity of adsorption.

The value of K_f and n (Table 3) were calculated from the linear plot of log q_e vs log C_e (Fig. 4b). The plot gives the values of n, lying between 1 and 10 which indicates the chemisorptions [76]. Isotherms with n>1 are classified as L-type isotherms reflecting a high affinity between adsorbate and adsorbent and are indicative of chemisorptions [77]. The Freundlich constant (K_f) which is related to the adsorption capacity, increased with temperature, indicating that the adsorption process is endothermic.

The Temkin isotherm model assumes that the adsorption energy decreases linearly with the surface coverage due to the adsorbent-adsorbate interactions. The linear form of the Temkin isotherm model [78] is illustrated below:

$$q_e = (\frac{RT}{b}) \log(AC_e) \quad (7)$$

Or $q_e = B \log A + B \log C_e$

Where; $B = \frac{RT}{b}$

b (J/mol) = Temkin constant, related to the heat of sorption.

A (L/g) = Temkin isotherm constant, also called equilibrium binding constant.

R = gas constant (8.314 J/mol K).

T (k) = absolute temperature.

From the linear plot of q_e vs log C_e (Fig. 4c), the correlation coefficients (R^2) >0.97 were computed at different temperatures for Temkin adsorption isotherm (which consider the chemisorptions of adsorbate onto the adsorbent). It revealed that the adsorption process follows the Temkin adsorption isotherm (Table 3) satisfactorily. This supports the findings that the adsorption of Cu (II) onto TiOSA is a chemisorption process [79-80].

The thermodynamic characteristic of a process is determined from the parameters such as enthalpy change ($\Delta H°$), free energy change ($\Delta G°$), entropy change ($\Delta S°$) and activation energy (E_a). If ΔG° value decreases with increasing temperature, the process will be spontaneous [81]. The thermodynamic study was carried out at 298, 303, and 308 K. The thermodynamic parameters were calculated based on the following equations:

$$\log b = \frac{\Delta S°}{R} - \frac{\Delta H°}{RT} = -\frac{\Delta G°}{RT} \quad (8)$$

$$\Delta G = \Delta H° - T\Delta S°$$

Where, b is the equilibrium constant, R is the universal gas constant (8.314 J/mol K), and T is the temperature (K). The positive enthalpy change (from Table 4; $\Delta H°$ = + 5.7875 kJ/mol) indicates the endothermic nature of the adsorption process. The positive entropy change ($\Delta S°$ = + 0.01867kJ/mol K) implies the increase of randomness at the solid/liquid interface during the adsorption of Cu (II) onto the TiOSA. The small free energy change ($\Delta G°$) which is decreasing with increasing temperature implies the favorable nature of the process.

Table 4. Values of thermodynamic parameters

Thermodynamic parameters					
Temp. (K)	ΔG^o (kJ/mol)	ΔH^o (kJ/mol)	ΔS^o(kJ /mol K)	E_a (kJ/mol)	S^*
298	0.22384	5.7875	0.01867	3.9	3.125×10^{-3}
303	0.13049				
308	0.03714				

Table 5. Values of R_L and χ^2 of Cu (II) adsorption onto TiOSA

Temp(K)	RL values					χ^2 values for Adsorption kinetics	
	5mg/L	10 mg/L	15 mg/L	20 mg/L	25 mg/L	Pseudo first order	Pseudo second order
298	0.1945	0.1077	0.0745	0.0569	0.0461		
303	0.1897	0.1048	0.0724	0.0553	0.0447	7.0371	0.6911
308	0.1685	0.0920	0.0633	0.0482	0.0389		

The following modified Arrhenius type equation, which is related to the surface coverage (θ), can express the sticking probability, S^* of an adsorbate on the adsorbent. This measures the potential of an adsorbate to remain on the adsorbent indefinitely [82] and the equation can be expressed as:

$$S^* = (1-\theta)\exp-(\frac{E_a}{RT}) \quad (9)$$

Or $\log(1-\theta) = \log S^* + \frac{E_a}{RT}$

Where, θ is surface coverage, E_a is the activation energy.

$$\theta = (1-\frac{C_e}{C_o})$$

Where, C_o and C_e are the initial and equilibrium Cu (II) concentrations respectively.

From the plot of $\log(1-\theta)$ vs 1/T with intercept $\log S^*$ and slope E_a/R, the value of S^* and E_a were calculated (Table 4). The value of S^* (3.125×10^{-3}) which is very close to zero, indicates that the adsorption mechanism follows chemisorptions and 3.9 kJ/mol is the activation energy (E_a) for the process [83].

The dimensionless equilibrium parameter (R_L) is one of the important characteristics of the Langmuir isotherm. The value of R_L provides valuable information on the adsorption isotherms process. The R_L is related with Langmuir isotherm constant by the following equation [78]:

$$R_L = \frac{1}{1+bC_o} \quad (10)$$

Where, b is the Langmuir isotherm constant and C_o is the initial Cu (II) concentration (mg/L).

If the condition is $0<R_L<1$, then the Langmuir isotherm is favorable; $R_L = 0$ and $R_L = 1$ give irreversible and linear isotherm respectively; whereas $R_L>1$ is unfavorable. The R_L values have been calculated at three different temperatures (Table 5) and the values are found to be in the range of 0.1945 to 0.0389, which implies that the Langmuir isotherm is favorable.

The Chi-square (χ^2) test analysis has been used to measure the difference between the experimental data and various models data. Mathematically, this can be expressed as:

$$\chi^2 = \sum\left[\frac{\left(q_{e.\exp} - q_{e.cal}\right)^2}{q_{e.cal}}\right] \quad (11)$$

Where, $q_{e.exp}$ is experimental equilibrium capacity data and $q_{e.cal}$ is the equilibrium capacity from a model. If the experimental data are similar to data from the model, the χ^2 value will be small and if they differ, χ^2 will be large [84].

For Pseudo first and Pseudo second-order kinetic models, the χ^2 values (Table 5) have been calculated. From the values, it is observed that χ^2 value (0.6911) concerning the Pseudo second-order kinetic model is smaller than that of the Pseudo first-order kinetic model. This means that

Cu (II) adsorption onto TiOSA preferably followed the Pseudo second-order kinetic model.

CONCLUSIONS

Surface modification of titanium dioxide (TiO_2) nanoparticles have been done by functionalization using succinic anhydride (SA) and studied the Cu (II) adsorption onto it. The study showed that the initial 15 mg/L Cu (II) can be reduced to less than 1.08 mg/L with an adsorbent dose of 0.6 g/50 mL at a contact time of 180 min. From the study, it is found that the removal efficiency of Cu (II) from water, in the case of TiOSA is higher than that of TiO_2. It was also found that the adsorption process preferably followed the Langmuir isotherm model and the adsorption data was found to be better fitted to the Pseudo second-order kinetic model. The study confirms that the TiOSA may be a useful adsorbent material for the removal of Cu (II) from water.

ACKNOWLEDGEMENTS

The authors are thankful to director DRL, for allowing carrying out part of the research work at DRL Tezpur. The authors also like to thank the water chemistry division of DRL Tezpur and Gauhati University for providing various instrumental facilities.

CONFLICTS OF INTEREST

The authors declare there are no conflicts of interest.

REFERENCES

1.Srivastava, Y. N. Environmental Pollution, Ashish Pub. House, New Delhi, 1995.

2.Dara, S. S. A Textbook of Environmental Chemistry and Pollution Control, New Delhi, Chand Publishing Company, India, Snoeink VL, Tenkin D, 1997.

3.Hawkins, D. T. Water Chemistry, John Wiley and Sons, Inc., New York, USA, 1983.

4.Tebbutt, T. H. Principles of Water Quality Control. 3rd Edn. Pergaman Press Oxford. 1983.

5. Rajkumar D, Kim J. Oxidation of various reactive dyes with in situ electro-generated active chlorine for textile dyeing industry wastewater treatment. Journal of Hazardous Materials. 2006;136(2):203-12.

6. Gómez-Álvarez A, Valenzuela-García JL, Meza-Figueroa D, de la O-Villanueva M, Ramírez-Hernández J, Almendariz-Tapia J, et al. Impact of mining activities on sediments in a semi-arid environment: San Pedro River, Sonora, Mexico. Applied Geochemistry. 2011;26(12):2101-12.

7. Afkhami A, Saber-Tehrani M, Bagheri H, Madrakian T. Flame atomic absorption spectrometric determination of trace amounts of Pb(II) and Cr(III) in biological, food and environmental samples after preconcentration by modified nano-alumina. Microchimica Acta. 2010;172(1-2):125-36.

8. Li Z, Chang X, Zou X, Zhu X, Nie R, Hu Z, et al. Chemically-modified activated carbon with ethylenediamine for selective solid-phase extraction and preconcentration of metal ions. Analytica Chimica Acta. 2009;632(2):272-7.

9. Marahel F, Ghaedi M, Montazerozohori M, Nejati Biyareh M, Nasiri Kokhdan S, Soylak M. Solid-phase extraction and determination of trace amount of some metal ions on Duolite XAD 761 modified with a new Schiff base as chelating agent in some food samples. Food and Chemical Toxicology. 2011;49(1):208-14.

10. Ayangbenro A, Babalola O. A New Strategy for Heavy Metal Polluted Environments: A Review of Microbial Biosorbents. International Journal of Environmental Research and Public Health. 2017;14(1):94.

11. Dixit R, Wasiullah, Malaviya D, Pandiyan K, Singh U, Sahu A, et al. Bioremediation of Heavy Metals from Soil and Aquatic Environment: An Overview of Principles and Criteria of Fundamental Processes. Sustainability. 2015;7(2):2189-212.

12. Gaur N, Flora G, Yadav M, Tiwari A. A review with recent advancements on bioremediation-based abolition of heavy metals. Environ Sci: Processes Impacts. 2014;16(2):180-93.

13. Tak HI, Ahmad F, Babalola OO. Advances in the Application of Plant Growth-Promoting Rhizobacteria in Phytoremediation of Heavy Metals. Reviews of Environmental Contamination and Toxicology: Springer New York; 2012. p. 33-52.

14. Kansal S, Singh M, Sud D. Studies on photodegradation of two commercial dyes in aqueous phase using different photocatalysts. Journal of Hazardous Materials. 2007;141(3):581-90.

15. Shen YF, Tang J, Nie ZH, Wang YD, Ren Y, Zuo L. Preparation and application of magnetic Fe3O4 nanoparticles for wastewater purification. Separation and Purification Technology. 2009;68(3):312-9.

16. España JS, Pamo EL, Pastor ES, Andrés JR, Rubí JAM. The Removal of Dissolved Metals by Hydroxysulphate Precipitates during Oxidation and Neutralization of Acid Mine Waters, Iberian Pyrite Belt. Aquatic Geochemistry. 2006;12(3):269-98.

17. da Fonseca MG, de Oliveira MM, Arakaki LNH, Espinola JGP, Airoldi C. Natural vermiculite as an exchanger support for heavy cations in aqueous solution. Journal of Colloid and Interface Science. 2005;285(1):50-5.

18.Wojtowicz, A.; Stoklosa, A., Removal of heavy metal ions on smectite ion-exchange column, *Pol. J. Environ. Stud.* 2002, 11 (1), 97-101.

19. Arous O, Gherrou A, Kerdjoudj H. Removal of Ag(l), Cu(II) and Zn(ll) ions with a supported liquid membrane containing cryptands as carriers. Desalination. 2004;161(3):295-303.

20. Öğütveren ÜB, Koparal S, Özel E. Electrodialysis for the removal of copper ions from wastewater. Journal of Environmental Science and Health Part A: Environmental Science and Engineering and Toxicology. 1997;32(3):749-61.

21. Hasan SH, Srivastava P. Batch and continuous biosorption of Cu2+ by immobilized biomass of Arthrobacter sp. Journal of Environmental Management. 2009;90(11):3313-21.

22. Sağ Y, Aktay Y. Kinetic studies on sorption of Cr(VI) and Cu(II) ions by chitin, chitosan and Rhizopus arrhizus. Biochemical Engineering Journal. 2002;12(2):143-53.

23. Zheng J-C, Feng H-M, Lam MH-W, Lam PK-S, Ding Y-W, Yu H-Q. Removal of Cu(II) in aqueous media by biosorp-

tion using water hyacinth roots as a biosorbent material. Journal of Hazardous Materials. 2009;171(1-3):780-5.
24. Feng Y, Gong J-L, Zeng G-M, Niu Q-Y, Zhang H-Y, Niu C-G, et al. Adsorption of Cd (II) and Zn (II) from aqueous solutions using magnetic hydroxyapatite nanoparticles as adsorbents. Chemical Engineering Journal. 2010;162(2):487-94.
25. Peng Q, Liu Y, Zeng G, Xu W, Yang C, Zhang J. Biosorption of copper(II) by immobilizing Saccharomyces cerevisiae on the surface of chitosan-coated magnetic nanoparticles from aqueous solution. Journal of Hazardous Materials. 2010;177(1-3):676-82.
26. Banerjee SS, Chen D-H. Fast removal of copper ions by gum arabic modified magnetic nano-adsorbent. Journal of Hazardous Materials. 2007;147(3):792-9.
27. Fu F, Wang Q. Removal of heavy metal ions from wastewaters: A review. Journal of Environmental Management. 2011;92(3):407-18.
28. Ahmed MJK, Ahmaruzzaman M. A review on potential usage of industrial waste materials for binding heavy metal ions from aqueous solutions. Journal of Water Process Engineering. 2016;10:39-47.
29. Barakat MA. New trends in removing heavy metals from industrial wastewater. Arabian Journal of Chemistry. 2011;4(4):361-77.
30. Jusoh A, Su Shiung L, Ali Na, Noor MJMM. A simulation study of the removal efficiency of granular activated carbon on cadmium and lead. Desalination. 2007;206(1-3):9-16.
31. Li K, Wang X. Adsorptive removal of Pb(II) by activated carbon prepared from Spartina alterniflora: Equilibrium, kinetics and thermodynamics. Bioresource Technology. 2009;100(11):2810-5.
32. Wu Q, Li W, Liu S. Carboxyl-rich carbon microspheres prepared from pentosan with high adsorption capacity for heavy metal ions. Materials Research Bulletin. 2014;60:516-23.
33. Chojnacki A, Chojnacka K, Hoffmann J, Górecki H. The application of natural zeolites for mercury removal: from laboratory tests to industrial scale. Minerals Engineering. 2004;17(7-8):933-7.
34. Jiang M-q, Jin X-y, Lu X-Q, Chen Z-l. Adsorption of Pb(II), Cd(II), Ni(II) and Cu(II) onto natural kaolinite clay. Desalination. 2010;252(1-3):33-9.
35.Tan, P.; Hu, Y.; Bi, Q. Competitive adsorption of Cu^{2+}, Cd^{2+} and Ni^{2+} from an aqueous solution on graphene oxide membranes, *Colloid Surf.* 2016, A 509, 56-64.
36. Ihsanullah, Abbas A, Al-Amer AM, Laoui T, Al-Marri MJ, Nasser MS, et al. Heavy metal removal from aqueous solution by advanced carbon nanotubes: Critical review of adsorption applications. Separation and Purification Technology. 2016;157:141-61.
37. Aman T, Kazi AA, Sabri MU, Bano Q. Potato peels as solid waste for the removal of heavy metal copper(II) from waste water/industrial effluent. Colloids and Surfaces B: Biointerfaces. 2008;63(1):116-21.
38. Guibal E. Interactions of metal ions with chitosan-based sorbents: a review. Separation and Purification Technology. 2004;38(1):43-74.
39. Hua M, Zhang S, Pan B, Zhang W, Lv L, Zhang Q. Heavy metal removal from water/wastewater by nanosized metal oxides: A review. Journal of Hazardous Materials. 2012;211-212:317-31.
40. Lee K, Baek M, Cho E, Park I. Magnetic separation and transfer of wastewater contaminants using magnetic travelling wave and micro magnetic bead. 2015 IEEE Magnetics Conference (INTERMAG); 2015/05: IEEE; 2015.
41. Huang Y, Keller AA. Magnetic Nanoparticle Adsorbents for Emerging Organic Contaminants. ACS Sustainable Chemistry & Engineering. 2013;1(7):731-6.
42. Su Y, Adeleye AS, Keller AA, Huang Y, Dai C, Zhou X, et al. Magnetic sulfide-modified nanoscale zerovalent iron (S-nZVI) for dissolved metal ion removal. Water Research. 2015;74:47-57.
43. Bagheri H, Afkhami A, Saber-Tehrani M, Khoshsafar H. Preparation and characterization of magnetic nanocomposite of Schiff base/silica/magnetite as a preconcentration phase for the trace determination of heavy metal ions in water, food and biological samples using atomic absorption spectrometry. Talanta. 2012;97:87-95.
44. Li Y, Zhu S, Liu Q, Chen Z, Gu J, Zhu C, et al. N-doped porous carbon with magnetic particles formed in situ for enhanced Cr(VI) removal. Water Research. 2013;47(12):4188-97.
45. Tang SCN, Lo IMC. Magnetic nanoparticles: Essential factors for sustainable environmental applications. Water Research. 2013;47(8):2613-32.
46. Hakami O, Zhang Y, Banks CJ. Thiol-functionalised mesoporous silica-coated magnetite nanoparticles for high efficiency removal and recovery of Hg from water. Water Research. 2012;46(12):3913-22.
47. Zhao Y-G, Shen H-Y, Pan S-D, Hu M-Q. Synthesis, characterization and properties of ethylenediamine-functionalized Fe3O4 magnetic polymers for removal of Cr(VI) in wastewater. Journal of Hazardous Materials. 2010;182(1-3):295-302.
48. Wang L, Li J, Jiang Q, Zhao L. Water-soluble Fe3O4 nanoparticles with high solubility for removal of heavy-metal ions from waste water. Dalton Transactions. 2012;41(15):4544.
49. Feng L, Cao M, Ma X, Zhu Y, Hu C. Corrigendum to "Superparamagnetic high-surface-area Fe3O4 nanoparticles as adsorbents for arsenic removal" [J. Hazard. Mater. 217–218 (2012) 439–446]. Journal of Hazardous Materials. 2012;227-228:484.
50. Singh S, Barick KC, Bahadur D. Surface engineered magnetic nanoparticles for removal of toxic metal ions and bacterial pathogens. Journal of Hazardous Materials. 2011;192(3):1539-47.
51. Zhang R, Wang X. One Step Synthesis of Multiwalled Carbon Nanotube/Gold Nanocomposites for Enhancing Electrochemical Response. Chemistry of Materials. 2007;19(5):976-8.
52. Gao T, Li Q, Wang T. Sonochemical Synthesis, Optical Properties, and Electrical Properties of Core/Shell-Type ZnO Nanorod/CdS Nanoparticle Composites. Chemistry of Materials. 2005;17(4):887-92.
53. Caruso F. Nanoengineering of Particle Surfaces. Advanced Materials. 2001;13(1):11-22.
54. Liao M-H, Chen D-H. Preparation and characterization of a novel magnetic nano-adsorbent. Journal of Materials Chemistry. 2002;12(12):3654-9.
55. Yu S-Y, Zhang H-J, Yu J-B, Wang C, Sun L-N, Shi W-D. Bifunctional Magnetic–Optical Nanocomposites: Grafting Lanthanide Complex onto Core–Shell Magnetic Silica Nanoarchitecture. Langmuir. 2007;23(14):7836-40.
56. Barick KC, Aslam M, Lin Y-P, Bahadur D, Prasad PV, Dravid VP. Novel and efficient MR active aqueous colloidal

Fe3O4 nanoassemblies. Journal of Materials Chemistry. 2009;19(38):7023.
57. Liu Z, Ding J, Xue J. A new family of biocompatible and stable magnetic nanoparticles: silica cross-linked pluronic F127 micelles loaded with iron oxides. New J Chem. 2009;33(1):88-92.
58. Chandra S, Mehta S, Nigam S, Bahadur D. Dendritic magnetite nanocarriers for drug delivery applications. New Journal of Chemistry. 2010;34(4):648.
59. Liu X, Hu Q, Fang Z, Zhang X, Zhang B. Magnetic Chitosan Nanocomposites: A Useful Recyclable Tool for Heavy Metal Ion Removal. Langmuir. 2008;25(1):3-8.
60. Yantasee W, Warner CL, Sangvanich T, Addleman RS, Carter TG, Wiacek RJ, et al. Removal of Heavy Metals from Aqueous Systems with Thiol Functionalized Superparamagnetic Nanoparticles. Environmental Science & Technology. 2007;41(14):5114-9.
61. Del Castillo PCH, Manuel SR, Ruiz F. An Easy and Efficient Method to Functionalize Titanium Dioxide Nanoparticles with Maleic Anhydride. Soft Nanoscience Letters. 2014;04(03):53-62.
62. Mugundan S, Rajamannan B, Viruthagiri G, Shanmugam N, Gobi R, Praveen P. Synthesis and characterization of undoped and cobalt-doped TiO2 nanoparticles via sol–gel technique. Applied Nanoscience. 2014;5(4):449-56.
63. León A, Reuquen P, Garín C, Segura R, Vargas P, Zapata P, et al. FTIR and Raman Characterization of TiO2 Nanoparticles Coated with Polyethylene Glycol as Carrier for 2-Methoxyestradiol. Applied Sciences. 2017;7(1):49.
64.Sridevi, D. V.; Ramesh, V.; Sakthivel, T.; Geetha, K.; Ratchagar, V. Synthesis, structural and optical properties of Co doped TiO_2 nanocrystals by Sol-Gel method, mechanics, *Materials Science & Engineering Journal, Magnolithe*, 2017, 9 (1).
65. Nyamunda BC, Chivhanga T, Guyo U, Chigondo F. Removal of Zn (II) and Cu (II) Ions from Industrial Wastewaters Using Magnetic Biochar Derived from Water Hyacinth. Journal of Engineering. 2019;2019:1-11.
66. Benzaoui T, Selatnia A, Djabali D. Adsorption of copper (II) ions from aqueous solution using bottom ash of expired drugs incineration. Adsorption Science & Technology. 2017;36(1-2):114-29.
67. Ugwu EI, Tursunov O, Kodirov D, Shaker LM, Al-Amiery AA, Yangibaeva I, et al. Adsorption mechanisms for heavy metal removal using low cost adsorbents: A review. IOP Conference Series: Earth and Environmental Science. 2020;614:012166.
68.Shuhaimen, M. S.; Abdulah, E. N.; Salim, R. M.; Samah, M. A. A.; Omar, M. N.; Ahmad, M. N. Adsorption study on the removal of copper ions from aqueous solution using sodium hydroxide-modified Carica papaya PEELS, *Malaysian Journal of Analytical Sciences*, 2019, 23 (6), 926 - 937.
69. Khandanlou R, Ahmad MB, Fard Masoumi HR, Shameli K, Basri M, Kalantari K. Rapid Adsorption of Copper(II) and Lead(II) by Rice Straw/Fe3O4 Nanocomposite: Optimization, Equilibrium Isotherms, and Adsorption Kinetics Study. PLOS ONE. 2015;10(3):e0120264.
70.Lagergren, S. About the theory of so called adsorption of soluble substances. *Ksver. Veterskapsakad. Handl.* 1898, 24, 1-39.
71. Ho Y-S. Second-order kinetic model for the sorption of cadmium onto tree fern: A comparison of linear and non-linear methods. Water Research. 2006;40(1):119-25.
72. Chien SH, Clayton WR. Application of Elovich Equation to the Kinetics of Phosphate Release and Sorption in Soils. Soil Science Society of America Journal. 1980;44(2):265-8.
73. Chowdhury S, Saha P. Sea shell powder as a new adsorbent to remove Basic Green 4 (Malachite Green) from aqueous solutions: Equilibrium, kinetic and thermodynamic studies. Chemical Engineering Journal. 2010;164(1):168-77.
74. Yang C-h. Statistical Mechanical Study on the Freundlich Isotherm Equation. Journal of Colloid and Interface Science. 1998;208(2):379-87.
75. Meenakshi S, Sundaram CS, Sukumar R. Enhanced fluoride sorption by mechanochemically activated kaolinites. Journal of Hazardous Materials. 2008;153(1-2):164-72.
76. Jiang J-Q, Cooper C, Ouki S. Comparison of modified montmorillonite adsorbents. Chemosphere. 2002;47(7):711-6.
77.Taha, M. R.; Ahmad, K.; Aziz, A. A.; Chik, Z. Geoenvironmental aspects of tropical residual soils. In: Huat, B. B. K., Gue, S. S.; Ali, F. H. (Ed). Tropical residual soils engineering, A. A. Balkema Publishers, London, UK, 2009, pp. 377-403.
78. Wang X-s, Qin Y. Equilibrium sorption isotherms for of Cu2+ on rice bran. Process Biochemistry. 2005;40(2):677-80.
79. Biswas K, Saha SK, Ghosh UC. Adsorption of Fluoride from Aqueous Solution by a Synthetic Iron(III)–Aluminum(III) Mixed Oxide. Industrial & Engineering Chemistry Research. 2007;46(16):5346-56.
80. Boparai HK, Joseph M, O'Carroll DM. Kinetics and thermodynamics of cadmium ion removal by adsorption onto nano zerovalent iron particles. Journal of Hazardous Materials. 2011;186(1):458-65.
81. Wan Ngah WS, Hanafiah MAKM. Adsorption of copper on rubber (Hevea brasiliensis) leaf powder: Kinetic, equilibrium and thermodynamic studies. Biochemical Engineering Journal. 2008;39(3):521-30.
82. Sundaram CS, Viswanathan N, Meenakshi S. Defluoridation chemistry of synthetic hydroxyapatite at nano scale: Equilibrium and kinetic studies. Journal of Hazardous Materials. 2008;155(1-2):206-15.
83. Horsfall Jnr M, Spiff AI. Effects of temperature on the sorption of Pb2+ and Cd2+ from aqueous solution by Caladium bicolor (Wild Cocoyam) biomass. Electronic Journal of Biotechnology. 2005;8(2):162-9.
84.Gandhi, M. R.; Kalaivani, G.; Meenakshi, S. Sorption of chromate and fluoride onto duolite A 171 anion exchange resin-a comparative study. *Elixir Poll.* 2011, 32, 2034-2040.